Electronic Supplementary Material (ESI) for Soft Matter.

Electronic Supplementary Information
Depletion-driven morphological transitions in hexagonal crystallites of virus rods

Baeckkyoung Sung,[1] Henricus Herman Wensink,[2] and Eric Grelet[1,*]

[1] *Centre de Recherche Paul-Pascal, UMR 5031, CNRS & Université de Bordeaux, 33600 Pessac, France*

[2] *Laboratoire de Physique des Solides, UMR 8502, CNRS & Université Paris-Sud, Université Paris-Saclay, 91405 Orsay, France*

[*] grelet@crpp-bordeaux.cnrs.fr;eric.grelet@crpp.cnrs.fr

I. SUPPLEMENTARY FIGURES

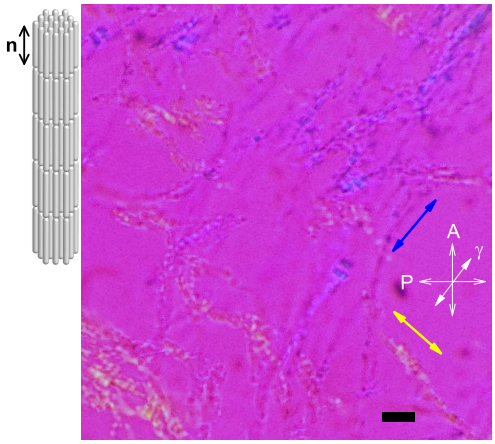

FIG. S1: Optical image of smectic fibers, where the sign of birefringence is verified with a full wavelength retardation plate, located between crossed polarizers (P and A). The retarded optical path results in fast (first order yellow) and slow (second order blue; marked by γ) axes in an isotropic medium (magenta background). The arrows represent the direction of the *fd* rods aligned parallel to the main axis (**n**) of the smectic fibers. Scale bar, 5 μm.

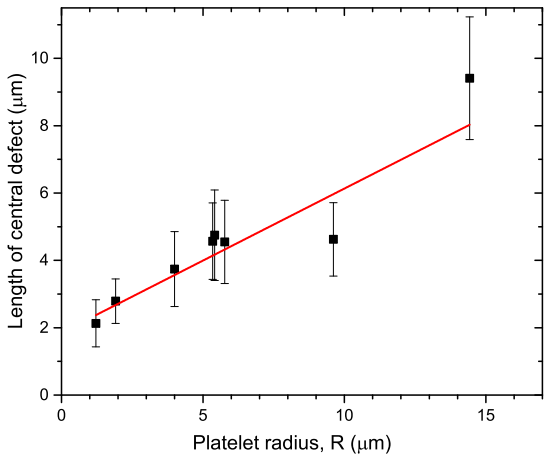

FIG. S2: Size of the central protruding defect as a function of the platelet diameter. A linear dependence is found, showing that the defect core reduces in size when the platelets become smaller. The smallest platelets show no discernible protrusions (defect length equal to platelet height) which enables them to stack on the top of each other forming smectic fibrils.

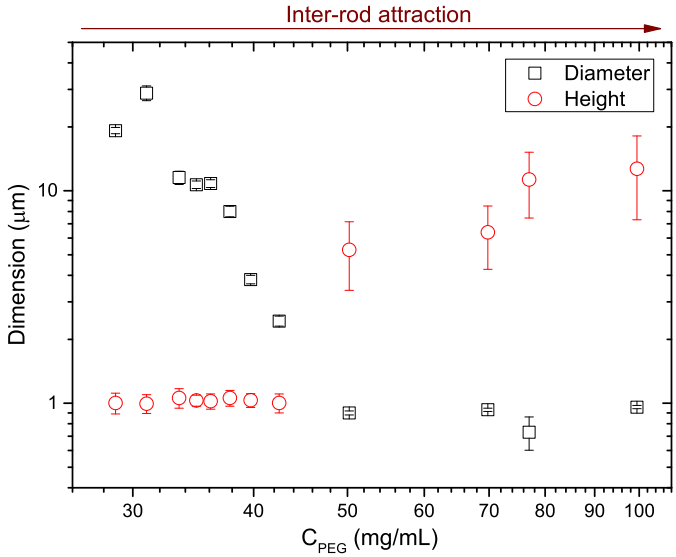

FIG. S3: Crossover from a 2D to 1D cluster morphology at increasing inter-rod attractions controlled by the PEG concentration (C_{PEG}) at a fixed rod concentration ($C_{fd-wt} = 10$ mg/mL). The variation of the cluster diameter (empty rectangles) and height (empty circles) enables a distinction between the different morphologies, as presented in Figure 3.

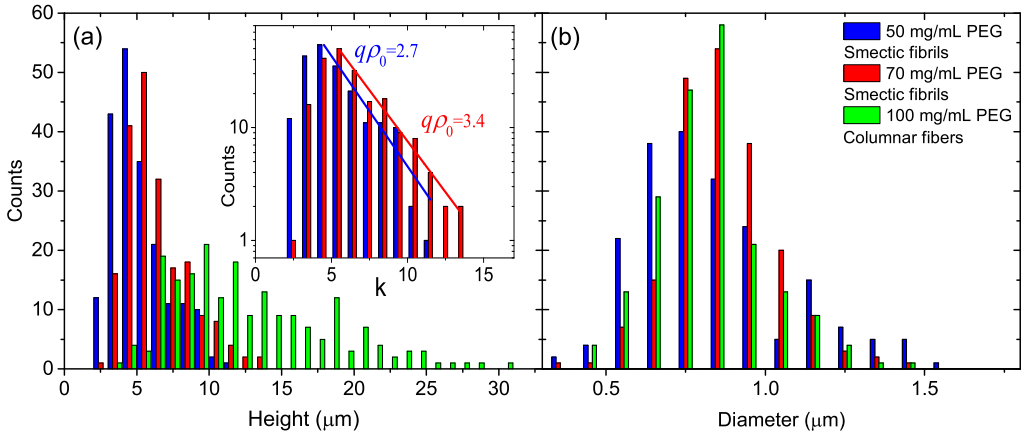

FIG. S4: Distributions of (a) heights, h, and (b) diameters, D, of the smectic fibrils (blue and red) and columnar bundles (green), for obtaining the mean values plotted in Figure S3. Inset: Log-lin representation of the smectic fibril degree of polymerization $k = h/\ell$, from which the fits (solid lines) using Eq. 16 provide $q\rho_0 = 2.7$ and 3.4 for C_{PEG} =50 and 70 mg/mL, respectively.

II. OSMOTIC PRESSURE FROM PEG SOLUTIONS (FIGURE 2B)

The osmotic pressure Π, in atm, is estimated according to the osmotic stress methods and is related to the PEG concentration C_{PEG}, in mg/mL, by using the following empirical relation [1]:

$$\Pi = -1.29G^2T + 127.6G^2 + 2.0G \tag{1}$$

with $G = C_{PEG}/(1000 - C_{PEG})$ and T the temperature, set at 22°C.

III. MODEL OF THE OSMOTIC PRESSURE APPLIED ON HEXAGONAL FD ARRAYS (FIGURE 2B)

In order to describe the osmotic pressure dependence of the charged viruses self-organized in a hexagonal lattice, a cylindrical cell model has been employed. In this model, a filamentous virus of bare radius $r = 3.5$ nm is surrounded by a cylindrical cell of diameter s, the interaxial rod distance, to account for the electric double layer. This yields a long-ranged electrostatic term $\Pi_e(s)$ of the the osmotic pressure, which is supplemented with a short-ranged repulsive hydratation contribution $\Pi_h(s)$. Both follow the same mathematical formulation and read up to leading order [2]:

$$\Pi(s) = \Pi_e(s) + \Pi_h(s) \tag{2}$$

where

$$\Pi_e(s) = A_e \left[K_0\left(\frac{s}{2\lambda_D}\right) / K_1\left(\frac{r}{\lambda_D}\right) \right]^2 \tag{3}$$

and

$$\Pi_h(s) = A_h \left[K_0\left(\frac{s}{2\lambda_h}\right) / K_1\left(\frac{r}{\lambda_h}\right) \right]^2 \tag{4}$$

Here $K_0(x)$ and $K_1(x)$ are the cylindrical modified Bessel functions of the second kind, and $\lambda_D = 0.9$ nm is the Debye screening length at ionic strength $I = 110$ mM. We fix the hydration repulsion length $\lambda_h = 0.25$ nm, according to the value found in literature [2, 3]. Upon fitting the data shown in Figure 2b, we obtain the values of both prefactors of Eqs. 3 and 4, $A_h \approx 175$ atm $\gg A_e \approx 175$ atm, which are consistent with those reported for DNA [2] and filamentous viruses [3].

IV. LINEAR REVERSIBLE POLYMERIZATION OF PLATELETS INTO SMECTIC FIBRILS

Let us consider a simple dynamical equilibrium whereby N_0 platelets (monomers) of thickness ℓ *reversibly* assemble into oligomers representing smectic fibrils of order $k = 1, 2, 3, ..., N_0$ and height $h = k\ell$. The formation and destruction of these k-mers is given by 'chemical reactions' described by:

$$kA_1 \underset{K_D}{\overset{K_A}{\rightleftharpoons}} A_k \tag{5}$$

where A_k denotes a $k-$mer of polymerization degree k, and K_A and K_D represent the association and dissociation rate constants, respectively. The rate of change of the $k-$mer concentration $[A_k]$ reads

$$\frac{d[A_k]}{dt} = K_A[A_1]^k - K_D[A_k] \tag{6}$$

Dynamic equilibrium ($d[A_k]/dt = 0$) leads to the law of mass-action:

$$K_{eq} \equiv \frac{K_A}{K_D} = \frac{[A_k]}{[A_1]^k} \tag{7}$$

in terms of the equilibrium constant K_{eq}. The statistical physics of chain formation driven by simple attractive bonds between adjacent monomers has been analyzed in detail in References [4–6]. In the case of ideal *non-interacting* filaments, the law of mass-action translates into a steady-state distribution $\rho_k = [A_k]$ of $k-$mers (number of aggregates per unit volume) taking the following form:

$$\rho_k = \rho_1(q\rho_1)^{k-1} \tag{8}$$

with ρ_1 the concentration of monomers, i.e. free unbonded platelets. The key parameter is the configuration integral q of a single depletion-driven bond which is defined as:

$$q \approx \exp(-\beta U_{\text{bond}}) \begin{cases} 0 & k_BT < U_{\text{bond}} \\ v_{ov} & k_BT > U_{\text{bond}} \end{cases} \tag{9}$$

Here, v_{ov} refers to the typical bonding volume which, assuming no other attractions than pure depletion, is expected to be of the order of the platelet surface times the depletion zone width R_g, i.e. $v_{ov} \sim R^2R_g$. Within this simple picture we find a monomer-only regime when the thermal energy $k_BT > U_{\text{bond}}$ and $\rho_k/\rho_1 \downarrow 1$, whereas at low temperature $k_BT < U_{\text{bond}}$ a broad distribution of $k-$mers appears. From the thermal volume of a single bond q we can

also determine the equilibrium constant of the reaction Eq. (5) via

$$K_{eq} \equiv \frac{K_A}{K_D} = (q\rho_0)^{k-1} \tag{10}$$

The normalization condition $\sum_{k=1}^{N_0} k\rho_k = \rho_0$ guarantees conservation of the total number of particles N_0 with ρ_0 the total monomer concentration. For $q\rho_1 < 1$ this leads to a closed expression for the aggregate distribution:

$$\rho_k = \frac{1}{q}\left(1 - \frac{2}{1+\sqrt{1+4q\rho_0}}\right)^k \tag{11}$$

From the average polymerization degree $\langle k \rangle$ we obtain the fibril aspect ratio (AR):

$$\mathrm{AR} \sim \frac{\ell\langle k \rangle}{2R_m} = \frac{\ell}{2R_m}(1+\sqrt{1+4q\rho_0}) \tag{12}$$

with R_m the minimal plate radius.

V. EFFECTIVE BOND ENERGY FOR SMECTIC FIBRILS

Let us assume the formation of platelets to follow some kind of diffusion-limited aggregation (DLA) process which proceeds on a time-scale much shorter than the typical polymerization time of the monomeric platelets. We further assume that the platelets are all equal in size and have a radius R_m in which case the core defect protrusions that prevent the platelets from binding together have vanished (Figure S2). The total number density of platelets ρ_0 formed is dictated by the total number of rods N_r in the system, as conservation of mass requires that $\rho_r \propto \rho_0 R_m^2 \ell \rho_c$ with ρ_c the number density of rods within the crystalline platelet, and ρ_r the overall rod concentration. The number density of platelets then scales as $\rho_0 \propto \phi_r/\phi_c \ell R_m^2$ in terms of the corresponding overall ("r") and intraplatelet ("c") volume fractions $\phi_{r/c} \sim \rho_{r/c}\pi r^2 \ell$. The aggregate thermal volume Eq. (9) can then be expressed as follows:

$$q\rho_0 \sim \frac{\phi_r}{\phi_c}\frac{r}{\ell}e^{-U_{\mathrm{bond}}/k_BT} \tag{13}$$

with $\phi_c \approx 0.5$ (corresponding to $C_{fd-wt} \approx 400$ mg/mL, see Figure 2a), $\phi_r \approx 0.01$ (corresponding to $C_{fd-wt} = 10$ mg/mL) and inverse rod aspect ratio $r/\ell \approx 0.04$. Here, we have tacitly assumed the bond energy U_{bond} to be larger than the thermal energy k_BT. The former is expected to increase with depletion strength and we conjecture:

$$\frac{U_{\mathrm{bond}}}{k_BT} \sim -C^*_{\mathrm{PEG}}\frac{v_{\mathrm{bond}}}{v_{\mathrm{pol}}} \tag{14}$$

in terms of the polymer (PEG) concentration $C^*_{\rm PEG} \sim P v_{\rm pol}$ renormalized to its overlap concentration. Here, $v_{\rm pol} \sim \frac{4\pi}{3} R_g^3$ represents the typical depletant volume. From Eq. (12),taking the monomer aspect ratio to be unity $\ell/2R_m \sim 1$ as experimentally observed, we infer that the fibril aspect ratio scales as:

$$\mathrm{AR} \sim 1 + \sqrt{1 + 4q\rho_0} \tag{15}$$

which enables a direct comparison with experimental data in Fig. 3. Values for $q\rho_0$ in the range from 2.7 to 3.4 can be extracted from the fibril length distribution ρ_k in Eq. (11) shown in Figure S4. To facilitate a fit with experimental data in the inset of Figure S4a, we recast the distribution Eq. (11) in exponential form, i.e.:

$$\rho_k \propto \exp\left(-\frac{2k}{1+\sqrt{1+4q\rho_0}}\right) \tag{16}$$

which is justified for $q\rho_0 > 1$. We estimate the typical bonding energy between the polymerizing platelets in the smectic fibrils to be about $U_{\rm bond} \sim -10 k_B T$ with the typical bonding volume between platelets lying in the range $v_{\rm bond} \sim 8 - 10 v_{\rm pol}$. Recalling Eq. (10) we can estimate the ratio of the association and dissociation rate constants of the reaction Eq. (5), leading to $K_A/K_D \sim 3^{k-1}$. This suggests that for long filaments ($k \gg 1$) dissociation events are much less frequent than bonding events, which is consistent with experimental findings where fibril dissocation is not observed on the probed time scale.

VI. SUPPLEMENTARY MOVIES

The Supplementary Movies show time-stream DIC/fluorescence overlaid images acquired simultaneously (See Methods) to monitor the dynamics of red fluorescent labeled viruses trapped in the self-assembled structures (platelets, smectic fibrils, and columnar fibers) of non-labeled viruses.

Movies S1-S2. Small hexagonal platelets displayed as individual objects (Movie S1) and as face-to-face stacks (Movie S2), with edge-on view. In the platelets, the labeled single viruses are aligned along the main platelet axis and exhibit no discernible self-diffusion along or normal to the main rod direction. Brownian motion of the stacked platelets can be observed in Movie S2. Scale bar, 1 μm.

Movies S3-S4. Side-view of smectic fibers. A single labeled virus rod (Movie S3) and a

labeled dimer virus (Movie S4) are incorporated within a single smectic-like layer (Movie S3) and in two adjacent smectic-like layers (Movie S4). These labeled viruses are aligned along the main cluster axis and do not show any self-diffusion along or normal to the rod direction. Scale bar, 1 μm.

Movie S5. Side-view of a columnar bundle. A labeled single virus is incorporated and aligns along the main axis of the bundle. This labeled virus does not show any self-diffusion along or normal to the main rod direction. Scale bar, 1 μm.

---

[1] C. B. Stanley and H. H. Strey, Measuring osmotic pressure of poly(ethylene glycol) solutions by sedimentation equilibrium ultracentrifugation, *Macromolecules*, 2003, **36**, 6888-6893.

[2] S. Yasar, R. Podgornik, J. Valle-Orero, M. R. Johmson and V. A. Parsegian, Continuity of states between the cholesteric-line hexatic transition and the condensation transition in DNA solutions, *Sci. Rep.*, 2014, **4**, 6877.

[3] G. Abramov, R. Shaharabani, O. Morag, R. Avinery, A. Haimovich, I. Oz, R. Beck and A. Goldbourt, Structural Effects of Single Mutations in a Filamentous Viral Capsid Across Multiple Length Scales, *Biomacromolecules*, 2017, **18**, 2258-2266.

[4] R. van Roij, Theory of Chain Association versus Liquid Condensation, *Phys. Rev. Lett.*, 1996, **76**, 3348.

[5] A. S. Perelson, F. W. Wiegel, The equilibrium size distribution of rouleaux, *Biophys J.*, 1982, **37**, 515-522.

[6] D. Frenkel and T. Schilling, Smectic filaments in colloidal suspensions of rods, *Phys. Rev. E*, 2002, **66**, 041606.